Published in final edited form as:
J Pathol. 2013 October ; 231(2): 223–235. doi:10.1002/path.4231.

Selective modulation through the glucocorticoid receptor ameliorates muscle pathology in *mdx* mice

Tony Huynh[1,3], **Kitipong Uaesoontrachoon**[1], **James L Quinn**[1], **Kathleen S Tatem**[1], **Christopher R Heier**[1], **Jack H Van Der Meulen**[1], **Qing Yu**[1], **Mark Harris**[2], **Christopher J Nolan**[3], **Guy Haegeman**[4], **Miranda D Grounds**[5], and **Kanneboyina Nagaraju**[1,*]

[1]Center for Genetic Medicine Research, Children's National Medical Center, Washington, DC, USA

[2]Department of Paediatric Endocrinology and Diabetes, Mater Children's Hospital, Brisbane, QLD, Australia

[3]Endocrine Research Unit and the Australian National University Medical School, Canberra Hospital, ACT, Australia

[4]Laboratory of Eukaryotic Gene Expression and Signal Transduction (LEGEST), University of Gent, Belgium

[5]School of Anatomy, Physiology and Human Biology, University of Western Australia, Perth, WA, Australia

Abstract

The over-expression of NF-κB signalling in both muscle and immune cells contribute to the pathology in dystrophic muscle. The anti-inflammatory properties of glucocorticoids, mediated predominantly through monomeric glucocorticoid receptor inhibition of transcription factors such as NF-κB (transrepression), are postulated to be an important mechanism for their beneficial effects in Duchenne muscular dystrophy. Chronic glucocorticoid therapy is associated with adverse effects on metabolism, growth, bone mineral density and the maintenance of muscle mass. These detrimental effects result from direct glucocorticoid receptor homodimer interactions with

*Correspondence to: Kanneboyina Nagaraju, Children's National Medical Center, 111 Michigan Avenue, N.W. Washington, DC 20010, USA. knagaraju@cnmcresearch.org.

Author contributions

TH, KU, CRH, MH, CJN, GH, MDG, and KN were involved in the conceptualization, design and planning of experiments; TH, KU, JLQ, KST, JHV, and QY were involved in performing the experiments; TH was the principle author of the manuscript; while KU, KST, CRH, MH, GH, MDG and KN provided editing support.

SUPPLEMENTARY MATERIAL ON THE INTERNET

The following supplementary material may be found in the online version of this article:

Supplementary Materials and Methods

Supplementary Results

Figure S1. Dose–response and cell viability curves in myoblasts and myotubes for CpdA and PNSL

Figure S2. Qualitative analysis using immunofluorescence of p65 nuclear translocation in H-2K mdx myoblasts and myotubes

Figure S3*Ex vivo* measurements of maximal isometric force, specific force and force following sequential lengthening–contractions in EDL muscles of WT and mdx mice

Table S1. Treatment groups for compound A efficacy trials

Table S2. qPCR reagents and thermal cycle conditions

Table S3. Primary and secondary antibodies used in western blot analysis

glucocorticoid response elements of the relevant genes. Compound A, a non-steroidal selective glucocorticoid receptor modulator, is capable of transrepression without transactivation. We confirm the *in vitro* NF-κB inhibitory activity of compound A in *H-2K*^{b}-tsA58 *mdx* myoblasts and myotubes, and demonstrate improvements in disease phenotype of dystrophin deficient *mdx* mice. Compound A treatment in *mdx* mice from 18 days of post-natal age to 8 weeks of age increased the absolute and normalized forelimb and hindlimb grip strength, attenuated cathepsin-B enzyme activity (a surrogate marker for inflammation) in forelimb and hindlimb muscles, decreased serum creatine kinase levels and reduced IL-6, CCL2, IFNγ, TNF and IL-12p70 cytokine levels in gastrocnemius (GA) muscles. Compared with compound A, treatment with prednisolone, a classical glucocorticoid, in both wild-type and *mdx* mice was associated with reduced body weight, reduced GA, tibialis anterior and extensor digitorum longus muscle mass and shorter tibial lengths. Prednisolone increased osteopontin (*Spp1*) gene expression and osteopontin protein levels in the GA muscles of *mdx* mice and had less favourable effects on the expression of *Foxo1*, *Foxo3*, *Fbxo32*, *Trim63*, *Mstn* and *Igf1* in GA muscles, as well as hepatic *Igf1* in wild-type mice. In conclusion, selective glucocorticoid receptor modulation by compound A represents a potential therapeutic strategy to improve dystrophic pathology.

Keywords

Duchenne muscular dystrophy; glucocorticoids; glucocorticoid receptor; transrepression NF-κB; compound A

Introduction

Duchenne muscular dystrophy (DMD) results from mutations in the *DMD* gene, located at Xp21.2 [1], and subsequent absence of the subsarcolemmal protein dystrophin [2,3]. Dystrophin is a component of the dystrophin–glycoprotein complex (DGC) that provides a scaffold between the extracellular matrix (ECM) and the cytoskeleton. Impaired DGC function compromises the structural and mechanical integrity of skeletal muscle, alters signalling pathways within the muscle, leading to contraction-induced injury, reduces cell viability and ultimately causes myofibre necrosis and muscle inflammation [4]. The nature and sequence of events that occur during the initiation and perpetuation of this inflammatory process in dystrophic muscle remains controversial. Glucocor-ticoids (GCs) are the only therapy shown to alter the natural history of DMD [2,3,5] and modulation of the inflammatory response is thought to underlie their efficacy. The anti-inflammatory properties of GCs are due to GC-bound glucocorticoid receptor (GR) monomer interference with pro-inflammatory transcription factors such as NF-κB (transrepression), whereas adverse metabolic alterations and detrimental changes in muscle and bone homeostasis [6] are due to GC-bound GR dimer interactions with GC response elements (GRE) mediating the transcription of the relevant genes (transactivation) [7].

In DMD, NF-κB, a transcription factor for many pro-inflammatory genes, promotes muscle damage and fibrosis, impairs myofibre regeneration and accelerates satellite cell senescence [8–11]. Numerous studies support targeting of NF-κB as a therapeutic approach in DMD [12–21]. Compound A (CpdA), or 2-(4-acetoxyphenyl)-2-chloro-*N* -methyl-ethylammonium

chloride [22]—a non-steroidal selective GR modulator (SGRM)—is the first natural compound with the ability to selectively induce GR-mediated transrepression. The molecular properties allowing CpdA to selectively signal through the GR, and its efficacy in animal models of inflammatory and immunological disorders, have been studied extensively [23–30]. CpdA has the theoretical potential to produce the beneficial effects of GCs in DMD, including NF-κB modulation [31], without the well-recognized adverse effects of GCs that often limit their therapeutic use. The aims of this study were to: test the beneficial potential of CpdA in the *mdx* mouse model of DMD; investigate the mechanisms by which these beneficial effects are achieved; and compare and contrast the effects of CpdA and prednisolone (PNSL), a classical GC, on mediators of muscle disease.

Materials and methods

Reagents/equipment were acquired through Life Technologies (Grand Island, NY, USA) unless stated otherwise. A complete description of the materials and methods is provided in the supplementary material.

Animals

Male wild-type (WT; *C57BL/10ScSn/J*) mice and *mdx* (*C57BL/10ScSn-mdx/J*) mice were obtained from the Jackson Laboratory (Bar Harbor, ME, USA) and housed/bred at the Veterans Affairs Animal Facility. All animal experiments were conducted in accordance with our IACUC guidelines under approved protocols.

Experimental design in animal studies and tissue preparation

All mouse studies followed a common schedule (Figure 1). Two studies were performed, with treatment groups outlined in Table S1 (see supplementary material). Intraperitoneal CpdA was favoured over oral CpdA because, at a dose of 7.5 mg/kg/day, intraperitoneal CpdA significantly reduced proinflammatory cytokine (IL-6, TNF, CCL2, IFNγ and IL-12p70) levels in gastrocnemius (GA) muscle. The 5.0 mg/kg/day dose of PNSL was chosen based on published FDA guidelines and our own experience with this dose in this model [32,33]. All animals were randomized to their treatment groups, based on body weight. Acquisition and analysis of all functional, imaging and histological data was performed in a blinded fashion.

Grip strength measurement (GSM)

Forelimb and hindlimb GSMs were performed as previously described [34], but with an increase in the acclimation period from 3 to 5 consecutive days. Absolute and normalized [to body weight (BW)] GSMs were measured.

Open-field behavioural activity

Voluntary locomotor activity was measured using an open-field behavioural activity assessment (Digiscan) apparatus (Omnitech Electronics, Columbus, OH, USA), as previously described [34]. Mice were acclimatized for 4 days before data collection every 10 min over a 1 h period each day for 4 consecutive days.

Measurement of histopathological parameters and serum creatine kinase (CK)

Assessment of pathology in WT and *mdx* mice following treatment was performed in paraffin-embedded right tibialis anterior (TA) cross-sections, using haema-toxylin and eosin (H&E) staining. Histological evaluations were performed in a blinded manner, using coded slides. Quantitative stereology was performed on a section of the entire TA (non-overlapping fields captured by a ×40 objective). Histological parameters were defined according to TREAT-NMD SOP criteria (Treat-NMD SOP No. DMD_M.1.2.007). CK determination was performed as previously described [34].

Quantitative real-time polymerase chain reaction (qPCR)

RNA was isolated from cells or frozen tissue using an integrated Trizol and RNeasy minikit (Qiagen, Valencia, CA, USA) protocol with DNase I treatment. cDNA was obtained using Reverse Transcription System (Promega, Madison, WI). All PCR reactions were carried out using Taqman Gene Expression Master Mix, except *Spp1* and *Hprt* gene analysis (SYBR Green PCR Master Mix). *Hprt* was used as the housekeeping gene in all qPCR studies. Relative quantification was used in all except in atrophy studies, where relative expression software tool (REST) was used. Comparisons were made between vehicle-treated WT and *mdx* mice as well as between the vehicle and other treatment groups. For studies of the expression of genes determining muscle mass, GA muscle was used for all genes except *Foxo3* , where the quadriceps was used due to inadequate mRNA from GA to complete all studies.

Taqman Gene Expression Assays, SYBR Green primer pairs, and thermal cycle conditions are presented in Table S2 (see supplementary material).

Flow cytometry

A fluorescence-activated cell sorting (FACS) system (BD Biosciences, San Jose, CA, USA) was used to quantify cytokines (IL-6, IL-10, CCL2, TNF, IFNγ, IL-12p70) in protein lysates from pulverized GA with the Cytometric Bead Array Mouse Inflammation Kit, measured according to the manufacturer's instructions.

Cell culture

Conditionally immortalized H-2kb-tsA58 (H-2k) *mdx* myoblasts were cultured as previously described [35,36]. The growth medium contained Dulbecco's modified Eagle's medium (DMEM), 20% fetal bovine serum (FBS), 2% chick embryo extract (US Biologicals, Boston, MA, USA), 2% L-glutamine, 1% penicillin/streptomycin and 0.02 μg/ml IFNγ (Millipore, Billerica, MA, USA) at 33°C with 10% CO_2. Differentiation into myotubes was achieved by removing the chick embryo extract, replacing the 20% FBS with 5% horse serum, and incubating at 37°C with 5% CO_2 for at least 96 h. AtT-20/D16v–F2 murine pituitary corticotrophs (ATCC, Manassas, VA, USA) were cultured as previously described [37].

Western blotting

H-2K *mdx* myoblasts were pretreated with 1% DMSO, CpdA (4 μM) or PNSL (10 μM) for 4 h, followed by stimulation with 10 ng/ml TNF for 30 min (non-stimulated DMSO-treated groups were also included). Myotubes were treated for 24 h before stimulation for 24 h. Nuclear and cytoplasmic fractions were then obtained, using a p65 (RelA) Translocation Assay Kit (Five Photons Biochemicals, San Diego, CA, USA) according to the manufacturer's instructions; 10 μl nuclear fraction and 15 μl cytoplasmic fraction from each treatment was used for the western blot, which was performed as previously described [38]. The primary and secondary antibodies used for immunoblotting are presented in Table S3 (see supplementary material). Densitometry analysis of p65 nuclear and cytoplasmic blots, normalized to both Actin and Lamin A, was used to assess p65 nuclear:cytoplasmic ratios.

Pituitary corticotroph studies

AtT-20 cells were treated with 1% DMSO, PNSL (1 or 10 μM) or CpdA (1 or 4 μM) for 24 h. The media were then collected for ACTH measurement with Mouse/Rat ACTH Ultra Sensitive lumELISA (Calbiotech, Spring Valley, CA, USA) according to the manufacturer's instructions. Each well was then washed with phosphate-buffered saline (PBS) before the addition of Trizol for RNA extraction.

Live animal optical imaging

Quantification of inflammation in limb muscles of mice was achieved using live-animal optical imaging of cathepsin-B enzyme activity, using a caged near-infrared substrate as previously described [39], with n =7–10/group.

Osteopontin (OPN) ELISA assay

Quantification of OPN in protein lysates from GA muscles was performed using a commercial kit (Mouse Osteopontin Quantikine ELISA Kit, R&D Systems, Minneapolis, MN, USA) according to the manufacturer's instructions.

Statistical analysis

Two-tailed Student's *t*-test was used for experiments involving two groups. One-way ANOVA with Dunnett's post-test comparison against a control was used for experiments involving more than two groups. Relative Expression Software Tool or non-parametric one-way ANOVA with a Kruskal–Wallis comparison of relative quantification (*RQ*) values were used for qPCR. Two-way ANOVA with Bonferroni post-test comparison with vehicle (VEH)-treated controls was performed in weekly BW measurements and lengthening–contraction studies involving different time points. The relationships between OPN levels and percentage necrotic fibres in the GA muscles of *mdx* mice were analysed using Pearson correlation. Significance was defined as $p < 0.05$. Prism 5 statistical software was used for analyses.

Results

In vitro studies

CpdA reduces TNF-induced p65 nuclear translocation in H-2K *mdx* muscle cells—Western blot analysis was used to assess the effect of CpdA on p65 nuclear translocation in pretreated H-2K *mdx* muscle cells in response to 10 ng/ml TNF stimulation (Figure 2A, B). The nuclear:cytoplasmic ratios were reduced by −80% in control DMSO-treated/non-TNF-stimulated (TNF^-) compared to DMSO-treated/TNF-stimulated (TNF^+) myoblasts, and by −40% in both CpdA-treated/TNF-stimulated (CpdA) and PNSL-treated/TNF-stimulated (PNSL) myoblasts compared with TNF^+ myoblasts. Lower ratios were also observed in myotubes: TNF^- (−75%), CpdA (−48%) and PNSL (−50.0%). Reduced TNF-induced p65 nuclear translocation in H-2K muscle cells following CpdA treatment was also demonstrated using immunofluorescence (Figure S2).

CpdA does not induce GR-related transactivation of genes—To confirm the absence of CpdA-induced GR–GRE interactions, we studied the effects of CpdA *in vitro* on the expression of *Pomc* and *Sgk1* [37]—genes involved in the hypothalamic–pituitary–adrenal (HPA) axis feedback regulation—in AtT-20/D16v–F2 cells (Figure 3A, B). *Pomc* gene expression was not downregulated by CpdA (at 4 or 1 μM), whereas PNSL at 10 and 1 μM decreased expression of *Pomc* by −60% and −63%, respectively (Figure 3A). Similarly, *Sgk1* gene expression was not different from control corticotrophs following CpdA treatment. PNSL at 10 and 1 μM up-regulated *Sgk1* gene expression by 11- and 8-fold, respectively. ACTH secretion by AtT-20/D16v–F2 cells (Figure 3C) was not changed following either CpdA treatments, whereas both PNSL concentrations reduced ACTH levels by approximately −70%. No dose–response effect was observed for *Pomc* or *Sgk1* gene expression or ACTH levels with PNSL.

In vivo studies with CpdA in *mdx* mice

The following results are described for study 1 and the experimental design is outlined in the supplementary material (Table S1, Figure S1).

CpdA does not alter tibial length or the normal pattern of BW gains in WT or *mdx* mice—Tibial length was used to assess the effects of drug treatment on long bone growth (Figure 4A, B). PNSL5.0 markedly reduced tibial length in both WT and *mdx* mice. This was not observed with CpdA7.5 treatment. The gain in BW of both WT and *mdx* mice (Figure 4C, D) treated with daily PNSL was reduced compared with the VEH-treated mice. In contrast, CpdA did not reduce BW gains except in *mdx* mice treated with CpdA7.5 at one single time point of 5 weeks.

CpdA increases GSMs in *mdx* mice—GSMs were performed at 6 weeks of age (Figure 5A – D). As expected, all GSM parameters were reduced in *mdx* compared to WT mice. In *mdx* mice, absolute and normalized forelimb GSMs were improved when compared to VEH treatment, following CpdA3.75 (+13% and +22%), CpdA7.5 (+21% and +30%) and PNSL5.0 (+15% and +50%) treatments. Improvement in absolute and normalized himdlimb GSM was also observed for *mdx* mice in the CpdA7.5 group (+19% and +28%), but only

normalized hindlimb was improved following CpdA3.75 (+19%) and PNSL5.0 (+40%) treatments. In WT mice, CpdA7.5 did not affect GSM, whereas PNSL5.0 improved normalized forelimb (+12%) but reduced absolute hindlimb (−13%). Ex vivo measurements of maximal isometric force, specific force, and force following sequential lengthening-contractions in the EDL muscles of both mdx and WT mice were not changed following CpdA treatment (Figure S3).

CpdA increases open-field locomotor activity in *mdx* mice—We used Digiscan to study the effects of CpdA on open-field behavioural activity. All measurement parameters were expressed as absolute values (Figure 5E – I). Quantification of horizontal activity, vertical activity and total distance over time for each mouse was obtained by normalizing to the movement time (Figure 5J – L). There was significant intragroup variation in all parameters. Differences were observed between WT and *mdx* mice, with WT mice having shorter rest times, greater horizontal activity and greater total distance. In WT mice, CpdA7.5 reduced horizontal activity and total distance. In *mdx* mice, the PNSL5.0-treated group had longer rest times. For the time that they were moving, WT mice exhibited greater horizontal and vertical activity than *mdx* mice. There was no difference in the distance/unit time between WT and *mdx* mice. CpdA and PNSL treatment in WT mice reduced total distance/s compared to the VEH-treated group. CpdA and PNSL treatment in *mdx* mice resulted in greater horizontal activity/s, but no difference in vertical activity/s or total distance/s.

CpdA reduces muscle inflammation in *mdx* mice—Muscle inflammation *in vivo* was quantified using live-animal optical imaging to measure photon intensity (an indicator of cathepsin-B enzyme activity) [39] in the limb muscles of *mdx* mice, using ProSense-680 (Figure 6). VEH-treated *mdx* mice had higher photon intensity measurements in both the forelimbs and hindlimbs when compared to VEH-treated WT mice. Treatment of *mdx* mice with CpdA7.5 and PNSL5.0 attenuated photon intensity in both the forelimb and hindlimb muscles when compared to VEH-treated *mdx* mice.

CpdA and PNSL effects on histopathological parameters in the TA muscle of *mdx* mice—Histological assessment of H&E sections were performed on the TA muscles harvested from 8 week-old *mdx* mice. Figure 7 shows representative H&E sections from the TA muscle and the percentage change (from the mean) in each parameter between VEH-treated *mdx* mice and the other *mdx* groups. Treatment with CpdA7.5 reduced degenerative myofibres (−52%), regeneration (−43%) and inflammatory infiltration (−55%). PNSL5.0 increased the percentage of degenerative fibres (+54%), which was associated with reduced regenerative fibres (−59%). Despite the increased necrosis, there was reduced inflammatory infiltration (−27%).

CpdA reduces inflammatory cytokine protein levels in GA muscles—The effects of CpdA and PNSL on inflammation in the muscles of *mdx* mice were quantified by analysing gene expression in GA muscles for the cytokines *Il6* , *Tnf* and *Ccl2* (Figure 8A). Gene expression was measured using qPCR and expressed as *RQ*. There were no differences in *RQ* between *mdx* mice groups for gene expression any of the cytokines. All genes

discriminated between VEH-treated WT and *mdx* mice. Protein levels of six inflammatory cytokines were measured in protein lysates from the same GA muscles via FACS (Figure 8B). IL-6, CCL2, TNF, IFNγ and IL-12p70 levels were all reduced in *mdx* mice treated with CpdA3.75, CpdA7.5 or PNSL5.0. IL-10 levels were not reduced in any of the treatment groups. All cytokines discriminated between VEH-treated WT and *mdx* mice, except for IL-10.

CpdA reduces serum CK levels in *mdx* mice—Serum CK levels were markedly elevated in VEH-treated *mdx* mice compared to VEH-treated WT mice (Figure 8C). Within the *mdx* mice groups, all treatments reduced serum CK levels when compared to VEH-treated *mdx* mice (CpdA3.75, −67%; CpdA7.5, −48%; PNSL5.0, −82%).

CpdA and PNSL have opposite effects on OPN protein levels in the GA muscles of *mdx* mice—To study the relationship between the effects of CpdA on OPN (*Spp1*) gene expression (Figure 8D) and protein levels (Figure 8E) in the GA muscles of *mdx* mice, we used qPCR and an OPN ELISA. OPN gene expression was down-regulated in *mdx* mice treated with CpdA7.5, but not with PNSL5.0. OPN protein levels were higher in the PNSL group compared to the CpdA group. Gene expression and protein levels of OPN were lower in VEH-treated WT mice compared to the VEH-treated *mdx* mice. There was a significant correlation between OPN protein levels in the GA muscles of and the percentage of necrotic myofibres in the TA muscles of *mdx* mice ($r^2 = 0.4147$, $p < 0.001$; Figure 8F).

CpdA does not affect the weights of the GA, TA and EDL muscles in *mdx* mice —PNSL5.0 reduced the weights of the GA, TA and EDL muscles in both WT (Figure 9A) and *mdx* mice (Figure 9B). CpdA7.5 did not cause any decrease in TA or EDL weights in either WT or *mdx* mice. The average weights of the GA (−23% and −29%) and TA (−21% and −22%) muscles were reduced in PNSL5.0-treated WT and *mdx* mice. The GA muscles of WT mice were also reduced (−8%) in the CpdA7.5 group, although this was not observed for CpdA in the *mdx* mice.

CpdA and PNSL have differential effects on the expression of atrophy-related genes in GA muscles of WT and *mdx* mice

To compare the effects of CpdA and PNSL in normal and dystrophic muscles, the expression of a number of atrophy-related genes was analysed by qPCR in GA muscles and liver of WT (Figure 9C) and *mdx* mice (Figure 9D). In WT mice, PNSL up-regulated *Foxo1* , *Foxo3*, *Fbxo32*, *Trim63* and *Mstn* mRNA, while down-regulating *Igf1* in both muscle and hepatic tissue. CpdA did not cause any changes to the expression of these genes in WT mice. In *mdx* mice, the effect of PNSL on the gene expression was less marked, with only up-regulation in *Foxo1* and *Foxo3* in muscle and down-regulation of hepatic *Igf1* . For CpdA, *Trim63* was down-regulated in *mdx* mice.

Discussion

This is the first study demonstrating the efficacy of CpdA in any muscle disease, including DMD. Previous studies have focused on its ability to inhibit NF-κB in immune cells. NF-κB

activation occurs via significantly different mechanisms in muscle and immune cells. Contraction-induced injury in muscle is one such example. CpdA possesses anti-inflammatory properties via selective transrepression through the GR. We have shown that CpdA is an inhibitor of NF-κB in both muscle *in vitro* (C2C12 and H-2K *mdx cells*) and immune cells *in vivo*. Our results support conclusions from previous studies [15] that confirm the contribution of NF-κB signalling to the pathogenesis of DMD.

In study 1, CpdA improved absolute and normalized GSM in the forelimbs and hindlimbs of *mdx* mice.

The improvements in absolute GSM were comparable to and, in the case of the hindlimb, better than that observed in the PNSL-treated group. PNSL5.0 increased necrosis in the TA and did not improve absolute GSM in the hindlimb. Weight-loss in PNSL-treated mice contributed to the perceived improvement in normalized GSM. There were no differences in *ex vivo* force contraction measurements using the EDL muscle. The difference in GSM and *ex vivo* force contraction results may reflect the relative contribution of different muscle groups in the performance of the GSM assay, and differences in the sensitivities of the assays. Moreover, GSM is dependent on behavioural aspects of the mice and CpdA may influence behaviour to improve performance in the GSM assay.

There were no statistical differences in histopathology between control and treatment *mdx* mice groups. The variation in the severity of pathology between individual mice and between muscles of the same *mdx* mouse [40], as well as the low-level chronic myonecrosis in untreated sedentary *mdx* mice [41], makes statistical comparison very difficult [34,42]. When comparing the mean values, differences were observed between findings in studies 1 and 2. PNSL increased necrosis and decreased regeneration in study 1, while reducing necrosis and increasing the number of regenerative fibres in study 2 (data not shown). CpdA reduced the amount of necrosis in both studies, but improved regeneration only in study 2. The recognized role that early inflammatory infiltration plays in the removal of necrotic myofibres and signalling for initiating regeneration may explain these differences [43]. In study 1, early PNSL and CpdA treatment may produce negative alterations in the signalling networks between muscle and immune cells to diminish regenerative capacity.

PNSL increased muscle necrosis in study 1, while reducing it in study 2. Some possible explanations include, for example, that mast cells rapidly accumulate and degranulate (by 8 h) in response to damage [40]. They play a pro-inflammatory role in the muscle of adult *mdx* mice [40,44,45] but their role in very young *mdx* muscles is not known. Nonetheless, the differential impact of PNSL and CpdA treatments on mast cell degranulation should be considered.

Neutrophil accumulation in damaged muscle occurs early to achieve debris removal and degradation at the site of injury. GCs, unlike CpdA, enhance neutrophil survival by modifying pro-apoptotic signals [46] and this may represent another potential advantage of CpdA and other SGRMs over GCs.

In damaged muscle, the macrophage population response transitions from Th-1-responsive promoting satellite cell activation and proliferation, while inhibiting differentiation, to Th-2-

responsive for differentiation, growth and repair [47–49]. Both CpdA and GCs inhibit the master Th-1 transcription factor, T-bet, by a transrepression mechanism [50]. However, GCs inhibit, while CpdA induces, GATA-3 (the master Th-2 transcription) activity, both via opposite effects on p38 MAPK-induced GATA-3 phosphorylation and its nuclear translocation [51]. While both GCs and CpdA ultimately favour a Th-2 over a Th-1 response, GCs achieve this via preferential inhibition of the Th-1 response while CpdA actively promotes the Th-2 response.

Muscle proteolysis through the ubiquitin– proteasome system is a dominant feature of GC-induced muscle atrophy preferentially affecting fast-twitch (type-II) muscle (GA, TA and EDL) fibres [52]. *Fbxo32* and *Trim63* are two ubiquitin ligases that target protein for degradation in the proteasome machinery and are up-regulated by GCs through *Foxo1* , a transcription factor serving as a major switch for enhanced atrophy-related gene expression. As expected, PNSL up-regulated *Foxo1* , *Foxo3* , *Fbxo32* and *Trim63* gene expression in WT GA muscles. CpdA did not alter the expression of these genes in WT or *mdx* mice. Interestingly, only *Foxo1* and *Foxo3* gene expression was increased in PNSL-treated *mdx* mice. Enhanced NF-κB activity independently causes muscle atrophy possibly through increased expression of *Trim63* [53,54]. NF-κB inhibition by PNSL in *mdx* GA muscles may account for the more favourable *Fbxo32* and *Trim63* gene expression profile observed in our study. The combined neutral effect of CpdA in normal muscle and inhibition of NF-κB in dystrophic muscle may explain the net down-regulation in *Trim63* gene expression in *mdx* mice. Muscle catabolism through the autophagy–lysosome pathway is mediated by *Foxo3* through Bnip3 [55]. The up-regulation of *Foxo3* by PNSL, and the associated increased autophagy, in both WT and *mdx* may represent a mechanism for the observed relative reduction in myofibre damage and inflammation.

Our results support previous studies confirming the pathological role of GC-induced augmentation of myostatin production in GC myopathy [56]. Myostatin negatively regulates muscle mass by inhibiting satellite cell proliferation and differentiation, reducing protein synthesis and altering muscle metabolism [57]. The up-regulation of *Mstn* gene expression by PNSL in WT mice was not observed with CpdA treatment. In sarcopenia, myostatin promotes the generation of ROS where NF-κB activity is elevated, and this is reversed in old *Mstn* null mice [58]. No differences were found in *Mstn* gene expression in the 8 week-old PNSL-treated and VEH-treated *mdx* mice in our study. NF-κB inhibition by PNSL may contribute to its neutral effect on *Mstn* gene expression in this group of mice.

IGF-1, produced predominantly in the liver but also in local tissues (muscle and bone), is a growth factor that stimulates myoblast proliferation and differentiation during myogenesis and muscle regeneration and mediates hypertrophy of growing myofibres [59,60]. GCs suppresses the GH–IGF-1 axis (resulting in reduced hepatic IGF-1 production) and also has a negative effect on muscle IGF-1 production [61]. IGF-1, in turn, plays a critical role in antagonizing the catabolic action of GCs [62]. In our study, PNSL reduced *IGF-1* gene expression in WT (liver and GA) and *mdx* mice (liver), while CpdA had no effect on *IGF-1* gene expression.

Increased OPN, predominantly from immune cells and myoblasts, is a striking feature of dystrophic muscles [63]. The presence of OPN appears to: correlate with necrosis [64]; be integral in the facilitation and modulation of the immune response; be essential for regeneration [65]; and mediate fibrosis [63]. In our study, OPN gene (*Spp1*) expression and protein levels in GA muscles were higher in *mdx* mice compared to WT mice. Interestingly, CpdA treatment in *mdx* mice, associated with reduced necrosis, reduced *Spp1* expression relative to VEH-treated *mdx* mice. In contrast, PNSL treatment was associated with more necrosis, unaltered *Spp1* and higher OPN protein level. Our results support a correlation (r^2 = 0.4147) between higher OPN levels and myonecrosis in dystrophic muscle.

We have demonstrated that selective signalling through the GR using CpdA modulates detrimental pathways such as NF-κB, while exerting positive influences on modifier genes (*Foxo1* , *Foxo3* , *Fbxo32* , *Trim63* , *Mstn*, *Igf1* and *Spp1*) and improving a range of outcome measures in *mdx* mice. Further studies investigating the relative contributions of GR signalling in dystrophic muscle would enhance our understanding of the disease and promote more targeted approaches to developing therapies.

Supplementary Material

Refer to Web version on PubMed Central for supplementary material.

Acknowledgments

The authors would like to thank Tanya Cohen, Will Coley, Arpana Sali and Aditi Phadke for technical assistance; and Jyoti Jaiswal and Will Coley for helpful discussions. KN is supported by the National Institutes of Health (2R24HD050846-06; R01-AR050478, 5U54HD053177 and K26OD011171), the Muscular Dystrophy Association (translational grant), the US Department of Defense (W81XWH-05-1-0616) and a pilot grant from Parent Project Muscular Dystrophy (PPMD). Tony Huynh would like to thank and acknowledge PPMD for providing the Peter B Weis-man Fellowship for the purposes of completing this work as part of his thesis.

References

1. Hoffman EP, Brown RH Jr, et al. Dystrophin: the protein product of the Duchenne muscular dystrophy locus. Cell. 1987; 51:919–928. [PubMed: 3319190]
2. Bushby K, Finkel R, Birnkrant DJ, et al. Diagnosis and management of Duchenne muscular dystrophy, part 1: diagnosis, and pharmacological and psychosocial management. Lancet Neurol. 2010; 9:77–93. [PubMed: 19945913]
3. Bushby K, Finkel R, Birnkrant DJ, et al. Diagnosis and management of Duchenne muscular dystrophy, part 2: implementation of multidisciplinary care. Lancet Neurol. 2010; 9:177–189. [PubMed: 19945914]
4. Gumerson JD, Michele DE. The dystrophin-glycoprotein complex in the prevention of muscle damage. J Biomed Biotechnol. 2011; 2011:210797. [PubMed: 22007139]
5. Manzur AY, Kuntzer T, Pike M, et al. Glucocorticoid corticosteroids for Duchenne muscular dystrophy. Cochrane Database Syst Rev. 2008:CD003725. [PubMed: 18254031]
6. Pivonello R, De Martino MC, De Leo M, et al. Cushing's syndrome. Endocrinol Metab Clin North Am. 2008; 37:135–149. ix. [PubMed: 18226734]
7. De Bosscher K, Haegeman G. Minireview: latest perspectives on antiinflammatory actions of glucocorticoids. Mol Endocrinol. 2009; 23:281–291. [PubMed: 19095768]
8. Evans NP, Misyak SA, Robertson JL, et al. Immune-mediated mechanisms potentially regulate the disease time-course of Duchenne muscular dystrophy and provide targets for therapeutic intervention. PMR. 2009; 1:755–768.

9. Monici MC, Aguennouz M, Mazzeo A, et al. Activation of nuclear factor-κB in inflammatory myopathies and Duchenne muscular dystrophy. Neurology. 2003; 60:993–997. [PubMed: 12654966]
10. Kumar A, Boriek AM. Mechanical stress activates the nuclear factor-KB pathway in skeletal muscle fibers: a possible role in Duchenne muscular dystrophy. FASEB J. 2003; 17:386–396. [PubMed: 12631578]
11. Messina S, Vita GL, Aguennouz M, et al. Activation of NF-κB pathway in Duchenne muscular dystrophy: relation to age. Acta Myol. 2011; 30:16–23. [PubMed: 21842588]
12. Reay DP, Yang M, Watchko JF, et al. Systemic delivery of NEMO binding domain/IKKy inhibitory peptide to young *mdx* mice improves dystrophic skeletal muscle histopathology. Neurobiol Dis. 2011; 43:598–608. [PubMed: 21624467]
13. Peterson JM, Kline W, Canan BD, et al. Peptide-based inhibition of NF-κB rescues diaphragm muscle contractile dysfunction in a murine model of Duchenne muscular dystrophy. Mol Med. 2011; 17:508–515. [PubMed: 21267511]
14. Tang Y, Reay DP, Salay MN, et al. Inhibition of the IKK/NF-kB pathway by *AAV* gene transfer improves muscle regeneration in older *mdx* mice. Gene Ther. 2010; 17:1476–1483. [PubMed: 20720575]
15. Acharyya S, Villalta SA, Bakkar N, et al. Interplay of IKK/NF-κB signaling in macrophages and myofibers promotes muscle degeneration in Duchenne muscular dystrophy. J Clin Invest. 2007; 117:889–901. [PubMed: 17380205]
16. Messina S, Bitto A, Aguennouz M, et al. The soy isoflavone genistein blunts nuclear factor-κB, MAPKs and TNFα activation and ameliorates muscle function and morphology in *mdx* mice. Neuromusc Disord. 2011; 21:579–589. [PubMed: 21658942]
17. Evans NP, Call JA, Bassaganya-Riera J, et al. Green tea extract decreases muscle pathology and NF-κB immunostaining in regenerating muscle fibers of *mdx* mice. Clin Nutr. 2010; 29:391–398. [PubMed: 19897286]
18. Siegel AL, Bledsoe C, Lavin J, et al. Treatment with inhibitors of the NF-κB pathway improves whole body tension development in the *mdx* mouse. Neuromusc Disord. 2009; 19:131–139. [PubMed: 19054675]
19. Pan Y, Chen C, Shen Y, et al. Curcumin alleviates dystrophic muscle pathology in *mdx* mice. Mol Cells. 2008; 25:531–537. [PubMed: 18460899]
20. Messina S, Bitto A, Aguennouz M, et al. Nuclear factor-KB blockade reduces skeletal muscle degeneration and enhances muscle function in *mdx* mice. Exp Neurol. 2006; 198:234–241. [PubMed: 16410003]
21. Messina S, Altavilla D, Aguennouz M, et al. Lipid peroxidation inhibition blunts nuclear factor-κB activation, reduces skeletal muscle degeneration, and enhances muscle function in *mdx* mice. Am J Pathol. 2006; 168:918–926. [PubMed: 16507907]
22. De Bosscher K, Van den Berghe W, Beck IM, et al. A fully dissociated compound of plant origin for inflammatory gene repression. Proc Natl Acad Sci USA. 2005; 102:15827–15832. [PubMed: 16243974]
23. Dewint P, Gossye V, De Bosscher K, et al. A plant-derived ligand favoring monomeric glucocorticoid receptor conformation with impaired transactivation potential attenuates collagen-induced arthritis. J Immunol. 2008; 180:2608–2615. [PubMed: 18250472]
24. Gossye V, Elewaut D, Van Beneden K, et al. A plant-derived glucocorticoid receptor modulator attenuates inflammation without provoking ligand-induced resistance. Ann Rheum Dis. 2009; 69:291–296. [PubMed: 19204014]
25. Gossye V, Elewaut D, Bougarne N, et al. Differential mechanism of NF-κB inhibition by two glucocorticoid receptor modulators in rheumatoid arthritis synovial fibroblasts. Arthritis Rheum. 2009; 60:3241–3250. [PubMed: 19877072]
26. Robertson S, Allie-Reid F, Vanden Berghe W, et al. Abrogation of glucocorticoid receptor dimerization correlates with dissociated glucocorticoid behavior of compound a. J Biol Chem. 2010; 285:8061–8075. [PubMed: 20037160]

27. van Loo G, Sze M, Bougarne N, et al. Antiinflammatory properties of a plant-derived, non-steroidal dissociated glucocorticoid receptor modulator in experimental autoimmune encephalomyelitis. Mol Endocrinol. 2010; 24:310–322. [PubMed: 19965930]
28. Reber LL, Daubeuf F, Plantinga M, et al. A dissociated glucocor-ticoid receptor modulator reduces airway hyperresponsiveness and inflammation in a mouse model of asthma. J Immunol. 2012; 188:3478–3487. [PubMed: 22393156]
29. Rauner M, Goettsch C, Stein N, et al. Dissociation of osteogenic and immunological effects by the selective glucocorticoid receptor agonist, compound A, in human bone marrow stromal cells. Endocrinology. 2011; 152:103–112. [PubMed: 21084452]
30. Rauch A, Gossye V, Bracke D, et al. An anti-inflammatory selective glucocorticoid receptor modulator preserves osteoblast differentiation. F A S E B J. 2011; 25:1323–1332.
31. De Bosscher K, Vanden Berghe W, Haegeman G. Crosstalk between nuclear receptors and nuclear factor-κB. Oncogene. 2006; 25:6868–6886. [PubMed: 17072333]
32. Reagan-Shaw S, Nihal M, Ahmad N. Dose translation from animal to human studies revisited. F A S E B J. 2008; 22:659–661.
33. Sali A, Guerron AD, Gordish-Dressman H, et al. Glucocorticoid-treated mice are an inappropriate positive control for long-term preclinical studies in the *mdx* mouse. PLoS One. 2012; 7:e34204. [PubMed: 22509280]
34. Spurney CF, Gordish-Dressman H, Guerron AD, et al. Preclinical drug trials in the *mdx* mouse: assessment of reliable and sensitive outcome measures. Muscle Nerve. 2009; 39:591–602. [PubMed: 19260102]
35. Morgan JE, Beauchamp JR, Pagel CN, et al. Myogenic cell lines derived from transgenic mice carrying a thermolabile T antigen: a model system for the derivation of tissue-specific and mutation-specific cell lines. Dev Biol. 1994; 162:486–498. [PubMed: 8150209]
36. Jat PS, Noble MD, Ataliotis P, et al. Direct derivation of conditionally immortal cell lines from an *H-2Kb-tsA58* transgenic mouse. Proc Natl Acad Sci USA. 1991; 88:5096–5100. [PubMed: 1711218]
37. Reiter MH, Vila G, Knosp E, et al. Opposite effects of serum- and glucocorticoid-regulated kinase-1 and glucocorticoids on POMC transcription and ACTH release. Am J Physiol Endocrinol Metab. 2011; 301:E336–E341. [PubMed: 21586695]
38. Rayavarapu S, Coley W, Cakir E, et al. Identification of disease specific pathways using *in vivo* SILAC proteomics in dystrophin-deficient *mdx* mouse. Mol Cell Proteom. 2013; 12:1061–1073.
39. Baudy AR, Sali A, Jordan S, et al. Non-invasive optical imaging of muscle pathology in *mdx* mice using cathepsin caged near-infrared imaging. Mol Imaging Biol. 2011; 13:462–470. [PubMed: 20661652]
40. Radley HG, Grounds MD. Cromolyn administration (to block mast cell degranulation) reduces necrosis of dystrophic muscle in *mdx* mice. Neurobiol Dis. 2006; 23:387–397. [PubMed: 16798005]
41. Grounds MD, Radley HG, Lynch GS, et al. Towards developing standard operating procedures for pre-clinical testing in the *mdx* mouse model of Duchenne muscular dystrophy. Neurobiol Dis. 2008; 31:1–19. [PubMed: 18499465]
42. Willmann R, De Luca A, Benatar M, et al. Enhancing translation: guidelines for standard pre-clinical experiments in *mdx* mice. Neuromuscul Disord. 2012; 22:43–49. [PubMed: 21737275]
43. Tidball, JG. Inflammation in skeletal muscle regeneration. In: Schiaffino, S., editor. In Skeletal Muscle Repair and Regeneration. Springer Science and Business Media; Dordrecht: 2008. p. 243-268.
44. Marques MJ, Ventura Machado R, Minatel E, et al. Disodium cromoglycate protects dystrophin-deficient muscle fibers from leak-iness. Muscle Nerve. 2008; 37:61–67. [PubMed: 17724738]
45. Granchelli JA, Avosso DL, Hudecki MS, et al. Cromolyn increases strength in exercised *mdx* mice. Res Commun Mol Pathol Pharmacol. 1996; 91:287–296. [PubMed: 8829768]
46. Saffar AS, Ashdown H, Gounni AS. The molecular mechanisms of glucocorticoids-mediated neutrophil survival. Curr Drug Targets. 2011; 12:556–562.
47. Serrano AL, Mann CJ, Vidal B, et al. Cellular and molecular mechanisms regulating fibrosis in skeletal muscle repair and disease. Curr To p D e v B i o l. 2011; 96:167–201.

48. Mann CJ, Perdiguero E, Kharraz Y, et al. Aberrant repair and fibrosis development in skeletal muscle. Skelet Muscle. 2011; 1:21. [PubMed: 21798099]
49. McLennan IS. Degenerating and regenerating skeletal muscles contain several subpopulations of macrophages with distinct spatial and temporal distributions. J Anat. 1996; 188(1):17–28. [PubMed: 8655404]
50. Liberman AC, Druker J, Refojo D, et al. Glucocorticoids inhibit GATA-3 phosphorylation and activity in T cells. FA S E B J. 2009; 23:1558–1571.
51. Liberman AC, Antunica-Noguerol M, Ferraz-de-Paula V, et al. Compound A, a dissociated glucocorticoid receptor modulator, inhibits T-bet (Th1) and induces GATA-3 (Th2) activity in immune cells. PLoS One. 2012; 7:e35155. [PubMed: 22496903]
52. Ruff RL, Weissmann J. Endocrine myopathies. Neurol Clin. 1988; 6:575–592. [PubMed: 3065602]
53. Cai D, Frantz JD, Tawa NE Jr, et al. IKKβ/NF-κB activation causes severe muscle wasting in mice. Cell. 2004; 119:285–298. [PubMed: 15479644]
54. Mourkioti F, Kratsios P, Luedde T, et al. Targeted ablation of IKK2 improves skeletal muscle strength, maintains mass, and promotes regeneration. J Clin Invest. 2006; 116:2945–2954. [PubMed: 17080195]
55. Mammucari C, Schiaffino S, Sandri M. Downstream of Akt: FoxO3 and mTOR in the regulation of autophagy in skeletal muscle. Autophagy. 2008; 4:524–526. [PubMed: 18367868]
56. Ma K, Mallidis C, Bhasin S, et al. Glucocorticoid-induced skeletal muscle atrophy is associated with upregulation of myostatin gene expression. Am J Physiol Endocrinol Metab. 2003; 285:E363–E371. [PubMed: 12721153]
57. Amthor H, Hoogaars WM. Interference with myostatin/ActRIIB signaling as a therapeutic strategy for Duchenne muscular dystrophy. Curr Gene Ther. 2012; 12:245–259. [PubMed: 22554312]
58. Sriram S, Subramanian S, Sathiakumar D, et al. Modulation of reactive oxygen species in skeletal muscle by myostatin is mediated through NF-κB. Aging Cell. 2011; 10:931–948. [PubMed: 21771249]
59. Clemmons DR. Role of IGF-I in skeletal muscle mass maintenance. Trends Endocrinol Metab. 2009; 20:349–356. [PubMed: 19729319]
60. Shavlakadze T, Chai J, Maley K, et al. A growth stimulus is needed for IGF-1 to induce skeletal muscle hypertrophy *in vivo* . J Cell Sci. 2010; 123:960–971. [PubMed: 20179101]
61. Gayan-Ramirez G, Vanderhoydonc F, Verhoeven G, et al. Acute treatment with corticosteroids decreases IGF-1 and IGF-2 expression in the rat diaphragm and gastrocnemius. Am J Respir Crit Care Med. 1999; 159:283–289. [PubMed: 9872851]
62. Schakman O, Gilson H, Kalista S, et al. Mechanisms of muscle atrophy induced by glucocorticoids. Horm Res. 2009; 72(suppl 1):36–41. [PubMed: 19940494]
63. Vetrone SA, Montecino-Rodriguez E, Kudryashova E, et al. Osteo-pontin promotes fibrosis in dystrophic mouse muscle by modulating immune cell subsets and intramuscular TGFβ. J Clin Invest. 2009; 119:1583–1594. [PubMed: 19451692]
64. Zanotti S, Gibertini S, Di Blasi C, et al. Osteopontin is highly expressed in severely dystrophic muscle and seems to play a role in muscle regeneration and fibrosis. Histopathology. 2011; 59:1215–1228. [PubMed: 22175901]
65. Uaesoontrachoon K, Wasgewatte Wijesinghe DK, Mackie EJ, et al. Osteopontin deficiency delays inflammatory infiltration and the onset of muscle regeneration in a mouse model of muscle injury. Dis Model Mech. 2012; 6:197–205. e-pub. [PubMed: 22917925]

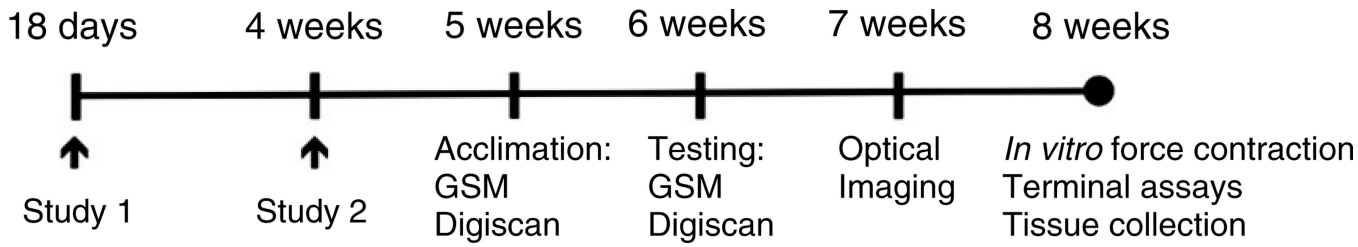

Figure 1.

Animal studies experimental design. Study 1 commenced at 18 days and study 2 at 4 weeks. Treatments were given daily and weights measured at commencement of study and then weekly. Studies 1 and 2 differ with regard to assays performed and numbers per group. GSM, grip strength measurement; Digiscan, open field behavioural activity measurements. Details of treatments of groups are provided in Table S1 (see Supplementary material)

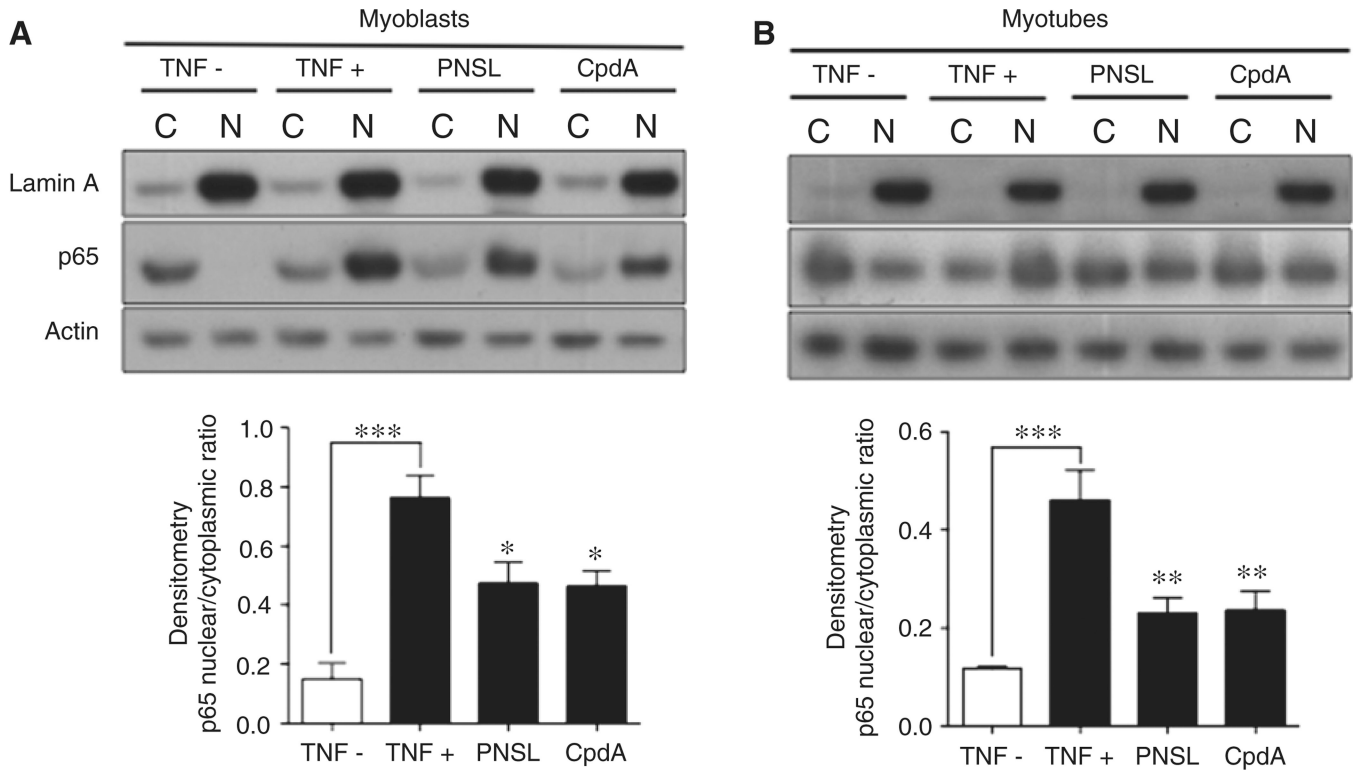

Figure 2.

Western blot with densitometry analysis of p65 nuclear translocation in H-2K mdx (A) myoblasts and (B) myotubes. CpdA reduces TNF-induced p65 nuclear translocation in H-2K *mdx* myoblasts and myotubes. H-2K muscle cells were pretreated with 1% DMSO, 10 μM PNSL or 4 μM CpdA before stimulation with 10 ng/ml TNF, as described in Materials and methods. The study included a DMSO-treated, non-stimulated control. A minimum of three independent experiments were performed. Densitometry measurements are expressed as mean ± SEM. Statistical analysis of densitometry was performed using one-way ANOVA and Dunnett's post-test comparison with the DMSO-treated, non-stimulated controls. TNF^{-}, DMSO-treated, non-stimulated; TNF^{+}, DMSO-treated, TNF-stimulated; PNSL, PNSL-treated, TNF-stimulated; CpdA, CpdA-treated, TNF-stimulated: $^{*}p < 0.05$; $^{**}p < 0.01$; $^{***}p < 0.001$

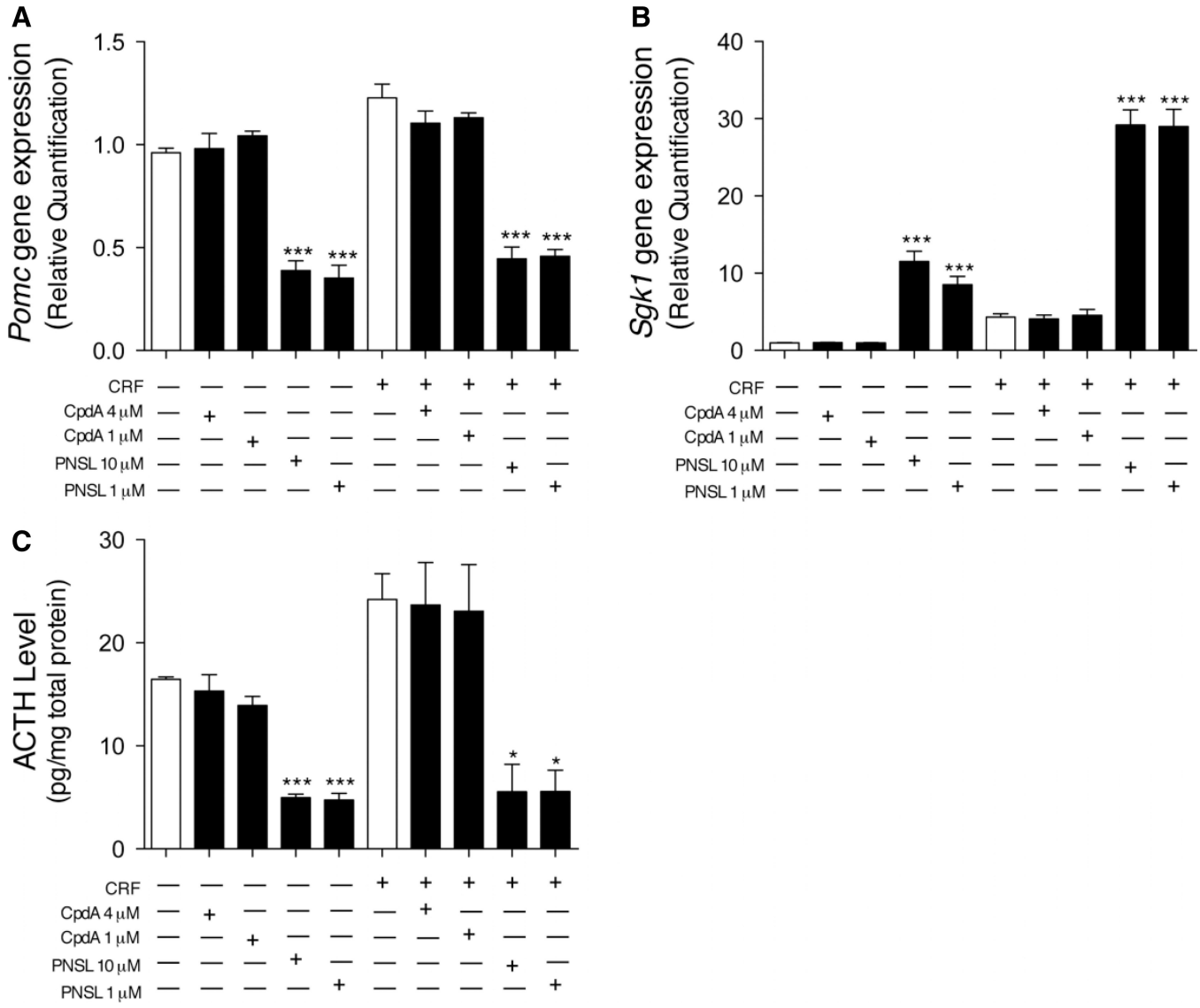

Figure 3.

(A) *Pomc* gene expression, (B) *Sgk1* gene expression and (C) media ACTH protein levels in experiments involving AtT-20/D16v–F2 pituitary corticotrophs. CpdA does not cause GR-related transactivation of genes (*Pomc* and *Sgk1*) involved in the feedback regulation of the hypothalamic–pituitary–adrenal (HPA) axis, and therefore preserves ACTH secretion in AtT-20/D16v–F2 murine corticotrophs. AtT-20/D16v–F2 cells were pretreated with 1% DMSO, 1 or 10 μM PNSL or 1 or 4 μM CpdA, as described in Materials and methods. Three independent experiments were performed for each study. Measurements are expressed as mean ± SEM; *$p < 0.05$; **$p < 0.01$; ***$p < 0.001$

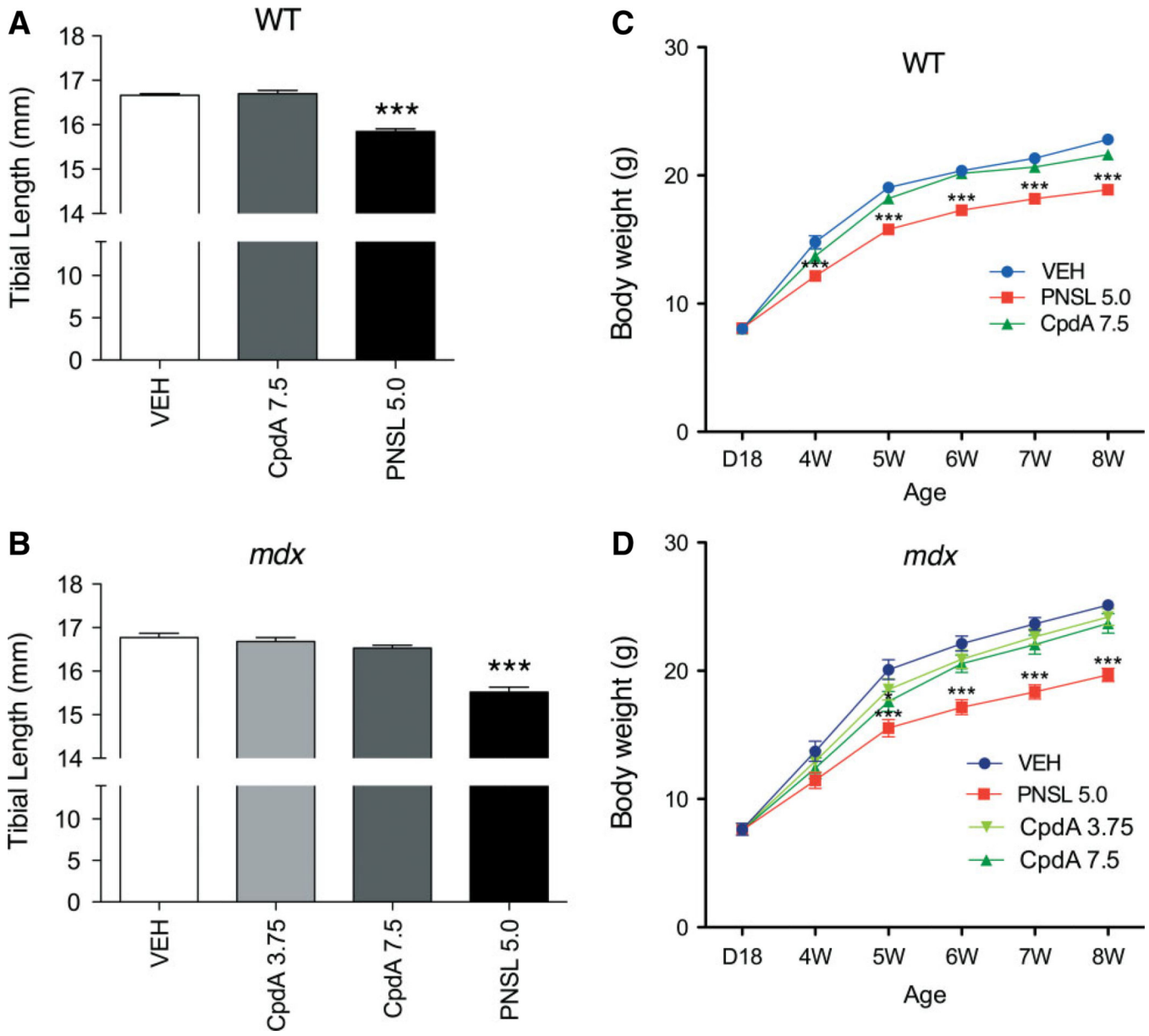

Figure 4.

(A, B) Tibial length and (C, D) weekly BWs were compared between CpdA and PNSL in WT and *mdx* mice, in both of which CpdA preserves long bone growth and patterns of weight gain. All comparisons were made with VEH-treated WT or *mdx* controls. In all analyses, $n = 15$/group. Measurements are expressed as mean ± SEM; all drug doses in mg/kg/day: $*p < 0.05$; $**p < 0.01$; $***p < 0.001$

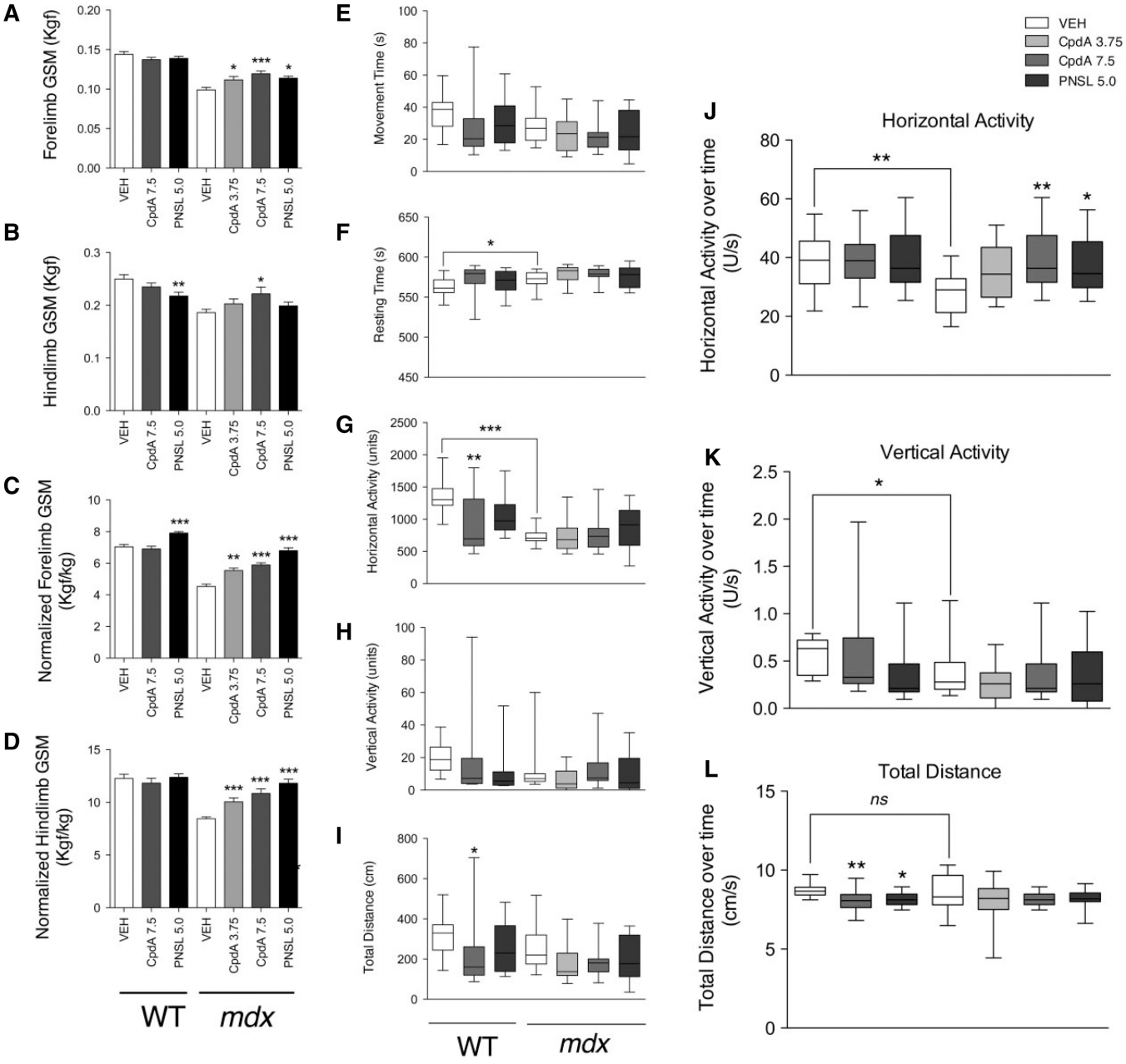

Figure 5.

(A–D) GSM, (E–I) absolute voluntary locomotor activity assessed by open-field behavioural activity measurements, and (J–L) voluntary locomotor activity normalized to movement time in WT and *mdx* mice. CpdA has positive effects on grip strength measurement (GSM) and voluntary locomotor activity. Absolute and normalized (to BW at the start of the testing period) strength was improved by intrperitoneal CpdA 7.5 mg/kg/day in both forelimbs and hindlimbs, while PNSL oral 5.0 mg/kg/day reduced absolute hindlimb GSM in WT mice. In *mdx* mice, CpdA 7.5 mg/kg/day increased the horizontal activity normalized for movement time. All comparisons were made with VEH-treated controls. Differences in all GSM parameters existed between WT and *mdx* mice. All measurements are expressed as mean ±

SEM; all groups, $n = 15$; all drug doses in mg/kg/day. See Materials and methods for details of drug treatments and GSM testing. GSMs were performed by the same individual, who was blinded to mouse strain and treatment group: *$p < 0.05$, **$p < 0.01$; ***$p < 0.001$

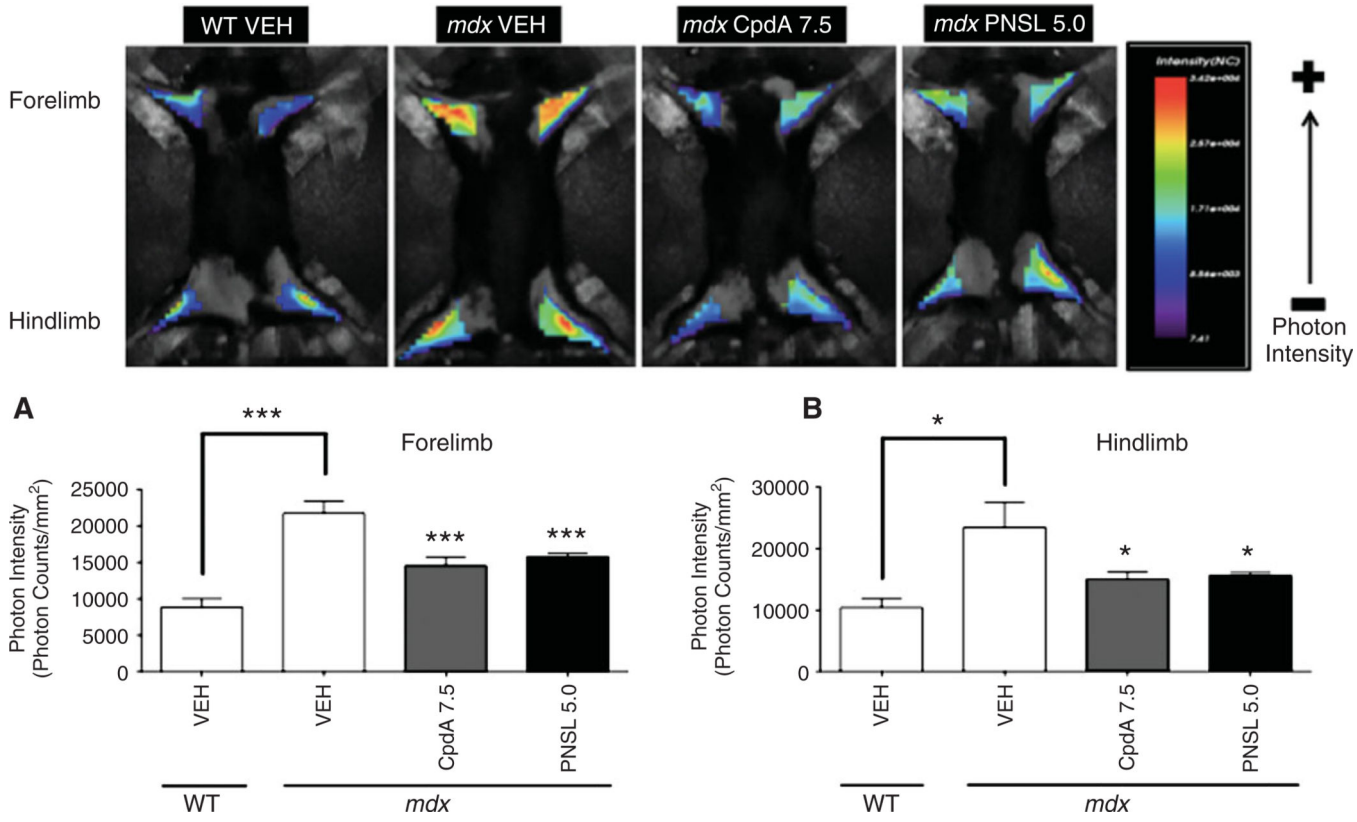

Figure 6.

Quantification of inflammation in (A) forelimb and (B) hindlimb muscles by measurement of cathepsin-B activity via live-animal optical imaging of WT and *mdx* mice. CpdA reduces photon intensity, a surrogate marker for inflammation, in both the forelimb and hindlimb muscles of *mdx* mice. Measurements were performed at 7 weeks of age and expressed as photon intensity (photon count/mm^2). Comparisons were made between VEH-treated WT and VEH-treated *mdx* groups. Within *mdx* groups, comparisons were made with the VEH-treated group. All measurements are expressed as mean ± SEM; WT VEH, $n = 7$; *mdx* VEH, $n = 8$; *mdx* CpdA 7.5, $n = 10$; *mdx* PNSL 5.0, $n = 9$; all drug doses in mg/kg/day: *$p < 0.05$; **$p < 0.01$; ***$p < 0.001$

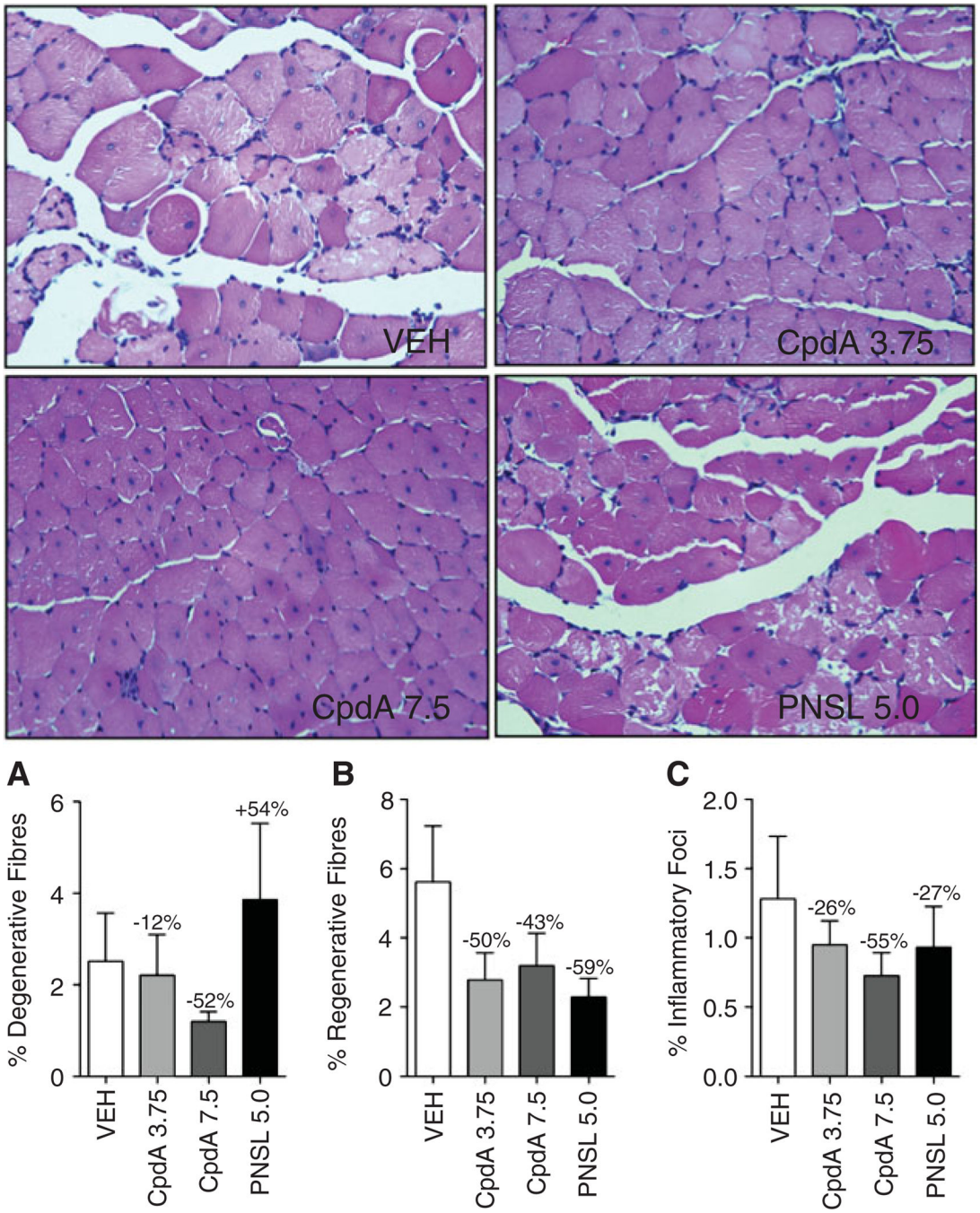

Figure 7.

Percentage of (A) degenerative fibres, (B) regenerative fibres and (C) inflammatory foci in the TA muscle of *mdx* mice, with representative H&E-stained sections from VEH-, CpdA- and PNSL-treated mice. CpdA did not improve histopathological parameters in the tibialis anterior (TA) muscles of *mdx* mice when treatment was commenced before the peak necrosis period (18 days). Comparisons were made with the VEH-treated group and percentage changes in parameters were calculated from the means. Histopathological parameters were scored on one cross-section of an entire TA at ×40 magnification in a

blinded fashion, using an accepted standard operating protocol from Treat-NMD, as described in Materials and methods. Measurements are expressed as mean ± SEM; all groups, $n = 12$; all drug doses in mg/kg/day: *$p < 0.05$; **$p < 0.01$; ***$p < 0.001$

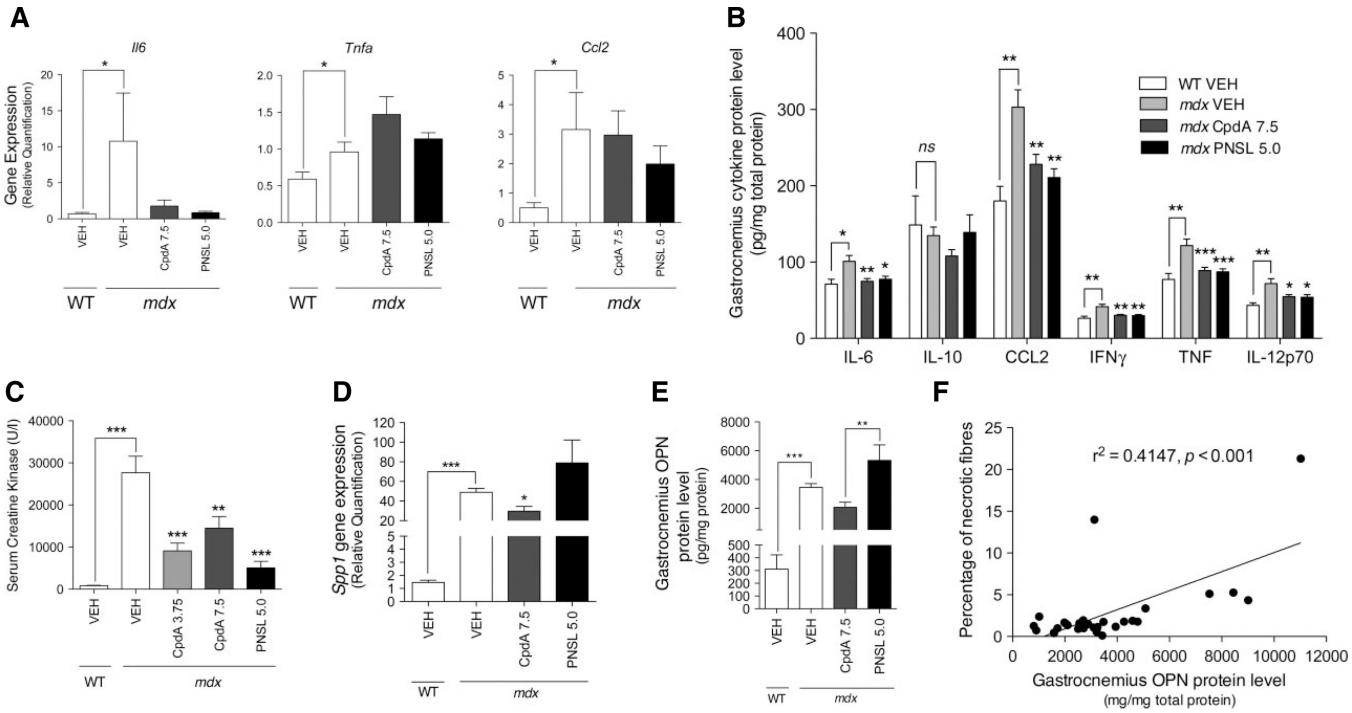

Figure 8.

(A) GA cytokine gene expression, (B) GA cytokine protein levels assessed via FACS, (C) serum CK levels, (D) GA *Spp1* gene expression, (E) GA OPN protein levels and (F) correlation between percentage degenerative fibres in the tibialis anterior and OPN protein levels in the GA were measured and calculated as described in Materials and methods. Inflammatory cytokine protein levels and osteopontin (OPN) gene (*Spp1*) expression in GA muscles, as well as serum creatine kinase (CK) levels, are reduced by CpdA in *mdx* mice. Comparisons were made between VEH-treated WT and VEH-treated *mdx* mice. Within the *mdx* groups, comparisons are made with the VEH-treated *mdx* group. Measurements are expressed as mean ± SEM; for CK levels, $n = 15$/group; cytokine gene expression, $n = 5$/group; cytokine protein levels, $n = 12$/group; OPN qPCR, WT, $n = 5$ and *mdx* groups, $n = 8$; OPN protein levels, WT, $n = 6$ and *mdx* groups, $n = 10$. All measurements are expressed as mean ± SEM; all drug doses in mg/kg/day: $^{*}p < 0.05$; $^{**}p < 0.01$; $^{***}p < 0.001$

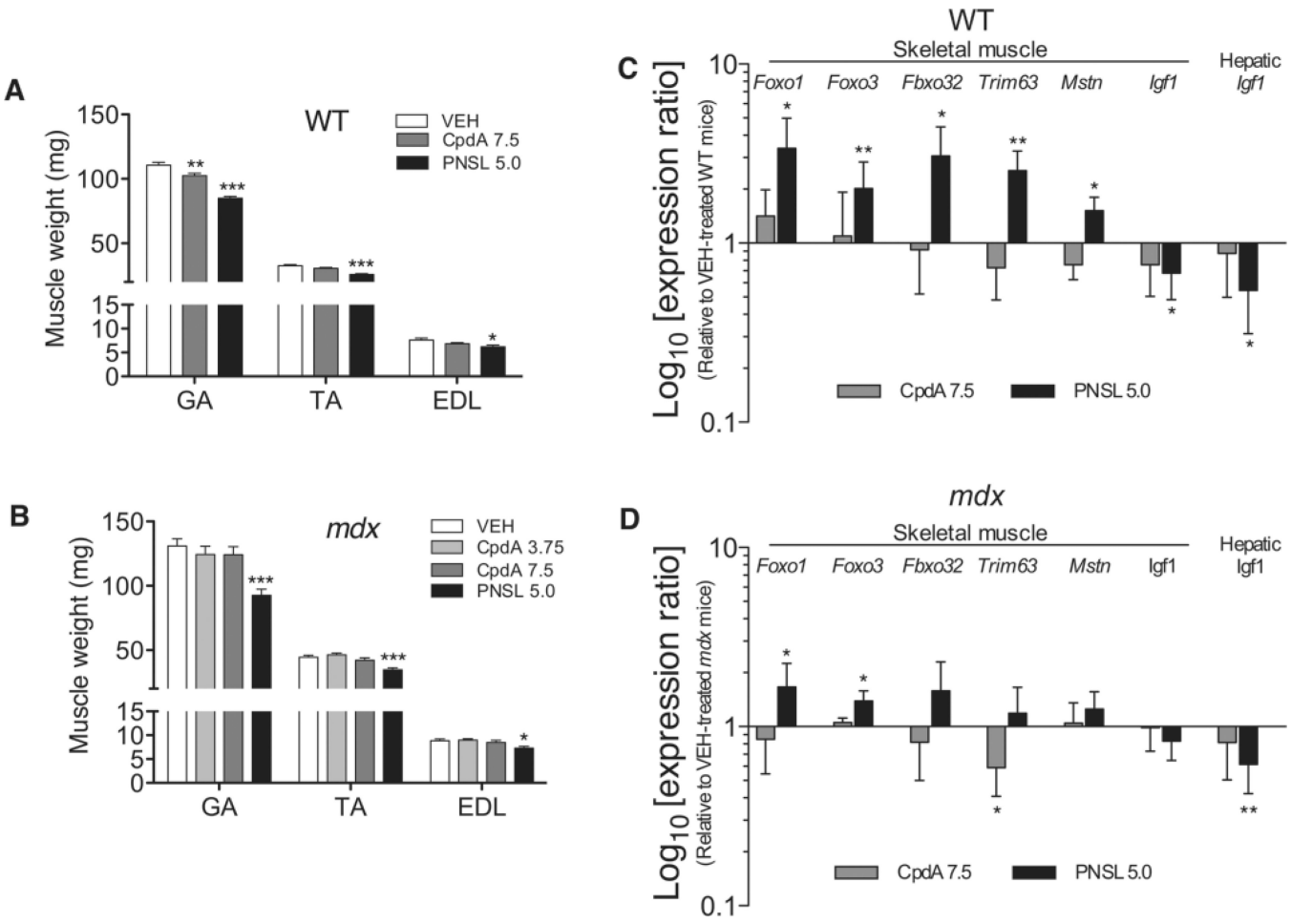

Figure 9.

(A, B) Muscle weights and (C, D) atrophy-related gene expression in gastrocnemius (GA) muscles (quadriceps muscles for *Foxo3* analysis) were compared in WT and *mdx* mice, in both of which CpdA has less effect on muscle mass and causes fewer adverse changes in the expression of genes related to the maintenance of muscle mass than PNSL. All comparisons are made with VEH-treated WT or *mdx* controls. In all analyses, $n = 15$/group, except in gene expression studies in GA muscles, where WT, $n = 5$ and *mdx*,$n = 8$–10. For *Foxo3* gene expression studies in quadriceps muscles, WT and *mdx*,$n = 8$ or 9. Measurements are expressed as mean ± SEM. GA and tibialis anterior (TA) weights were an average of both left and right muscles, while extensor digitorum longus (EDL) weights were only taken from the left muscle, due to use of the right EDL for *in vitro* force contraction studies. All drug doses in mg/kg/day: $^{*}p < 0.05$; $^{**}p < 0.01$; $^{***}p < 0.001$